Journal of Hazardous Materials 217–218 (2012) 123–132

Contents lists available at SciVerse ScienceDirect

Journal of Hazardous Materials

journal homepage: www.elsevier.com/locate/jhazmat

The investigation of kinetic and isotherm of fluoride adsorption onto functionalize pumice stone

Ghorban Asgari [a], Babak Roshani [b,*], Ghader Ghanizadeh [c]

[a] Department of Environmental Health Engineering, School of Health, Hamadan University of Medical Sciences, Hamadan, Iran
[b] Department of Chemical and Biological Engineering, University of Saskatchewan, 57 Campus Drive, Saskatoon, SK, S7N 5A9, Canada
[c] Health Research Center and Health School, Baqiyatallah University of Medical Sciences, Tehran, Iran

ARTICLE INFO

Article history:
Received 7 October 2011
Received in revised form 25 January 2012
Accepted 2 March 2012
Available online 23 March 2012

Keywords:
Pumice
Adsorption
Fluoride
Drinking water
Hexadecyltrimethyl ammonium

ABSTRACT

In this research work, pumice that is functionalized by the cationic surfactant, hexadecyltrimethyl ammonium (HDTMA), is used as an adsorbent for the removal of fluoride from drinking water. This work was carried out in two parts. The effects of HDTMA loading, pH (3–10), reaction time (5–60 min) and the adsorbent dosage (0.15–2.5 g L^{-1}) were investigated on the removal of fluoride as a target contaminate from water through the design of different experimental sets in the first part. The results from this first part revealed that surfactant-modified pumice (SMP) exhibited the best performance at dose 0.5 g L^{-1}, pH 6, and it adsorbs over 96% of fluoride from a solution containing 10 mg L^{-1} fluoride after 30 min of mixing time. The four linear forms of the Langmuir, Freundlich, Temkin and Dubinin–Radushkevich isotherms model were applied to determine the best fit of equilibrium expressions. Apart from the regression coefficient (R^2), four error functions were used to validate the isotherm and kinetics data. The experimental adsorption isotherm complies with Langmuir equation model type 1. The maximum amount of adsorption (Q_{max}) was 41 mg g^{-1}. The kinetic studies indicated that the adsorption of fluoride best fitted with the pseudo-second-order kinetic type 1. Thermodynamic parameters evaluation of fluoride adsorption on SMP showed that the adsorption process under the selected conditions was spontaneous and endothermic. The suitability of SMP in defluoridation at field condition was investigated with natural groundwater samples collected from a nearby fluoride endemic area in the second part of this study. Based on this study's results, SMP was shown to be an affordable and a promising option for the removal of fluoride in drinking water.

1. Introduction

Fluoride is the first element of the halogen family in the periodic table that does not occur in the element state in the environment due to its high reactivity [1]. The presence of fluoride in drinking water in acceptable concentrations is known as an essential constituent for human health, especially in children below 8 years of age [2]. However, when fluoride concentration exceed the acceptable level (1.5 mg L^{-1}), it leads to serious health problems such as skeletal fluorosis, mottling of teeth and lesions of endocrine glands, thyroid, liver and some other organs. Fluoride compounds are used in industry for a wide range of applications, such as: aluminum production, glass fiber [3], phosphate fertilizers, bricks, tiles, ceramics [3,4], drinking water fluoridation and toothpaste [5]. Weathering of rocks and industrial discharges are the main sources of fluoride in water, air, and soil [1]. In some provinces of Iran, the level of fluoride in drinking water is greater than 1.5 mg L^{-1}, which can lead to endemic fluorosis. This problem is visible in several countries, including China, the United States, Tanzania, Mexico, Kenya, Poland and Pakistan [2]. The levels of human daily exposure/intake of fluoride mainly depend on the geographical conditions and lifestyles [6]. Potable water is the main source of fluoride intake in humans. As previously stated, water in many places of the world contains high concentrations of permissible fluoride ions. Therefore, treatment of fluoride-contaminated water to a level below the permissible value that is recommended by the WHO has become a critical health issue.

Several methods, such as reverse osmosis, ion exchange/adsorption, coagulation, precipitation, and electro coagulation have been used for the removal of excess fluoride from drinking water [7–9]. Among these methods, adsorption is the most extensively used and is a promising technique for the removal of fluoride. A large number of materials such as activated alumina, red mud, quartz, and fly ash have been suggested for the adsorption of fluoride from water [2,10–12]. However, in recent

* Corresponding author. Tel.: +1 438 837 5468; fax: +1 306 966 4777.
E-mail address: babak.roshani@gmail.com (B. Roshani).

0304-3894/$ – see front matter © 2012 Elsevier B.V. All rights reserved.
doi:10.1016/j.jhazmat.2012.03.003

years, studies have been devoted to low-cost materials such as local mineral sorbents for the elimination of pollutants from water. These sorbents can be used in natural or modified forms. One such low-cost material is pumice [13–16].

Pumice is a light, porous, volcanic stone with a large surface area. It is easily and cheaply found in nature or some kinds of waste. Pumice is composed of highly microvesicular glass pyroclastic with very thin, translucent bubble walls of extrusive igneous rock. Pumice is commonly pale in color, ranging from white, cream, blue, or grey, to green-brown or black. It is formed when volcanic gases exsolving from viscous magma nucleate bubbles, which cannot readily decouple from the viscous magma prior to chilling to glass [16,17]. It is a common product of explosive eruptions (plinian and ignimbrite-forming) and commonly forms zones in upper parts of silicic lavas. Pumice has an average porosity of 90%, and initially floats on water [18–21].

Pumice has been widely tested and used in water treatment as an adsorbent, filter bed and support media [17,18,20]. Akbal studied the adsorption of phenol and 4-chlorophenol onto surfactant-modified and unmodified pumice from an aqueous solution. Experimental results showed that unmodified pumice cannot adsorb the phenol compound, but modified pumice is an excellent adsorbent of phenol and 4-chlorophenol [22]. Since pumice is a low-cost material with a porous structure and a large surface area widely available and easily processed and modified, thus modified pumice stone would be a suitable candidate as an adsorbent.

Due to the aforementioned advantage of original and modified pumice, to develop its application for removal of pollutant, it is very beneficial to study the performance of surfactant-modified pumice in eliminating other contaminates, such as fluoride. As mentioned above, several methods and many adsorbents in literature have been used to remove fluoride from water; however, to our knowledge from reviewing the literature, pumice and surfactant-modified pumice used for fluoride removal have not yet been reported. Accordingly, in this work, the capabilities of pumice and surfactant-modified pumice were evaluated in the removal of fluoride from water. The main aim of this study is to demonstrate the performance capacity of modified pumice to adsorb fluoride from drinking water. A series of experiments such as surfactant loading, pH, adsorbent dosage, contact time, and environmental water quality was carried out to investigate their effects on the fluoride adsorption capacity of modified pumice. The kinetics and isotherms of fluoride adsorption with modified pumice stone were also studied.

2. Materials and methods

2.1. Sorbent

Pumice stone was supplied from Tikmadash mine, located in the south of East Azerbaijan province, in the northwestern area of Iran. It was washed with distilled water several times and dried out at room temperature. The desired particle size (mesh 80–100) of pumice was obtained from sieve pumice, which had been grinded previously. The characteristics of the natural pumice and its modified form were determined by evaluating surface morphology, specific surface area, pore size and volume, and electrokinetic properties. The surface structures of natural and modified pumice particles were analyzed using a Philips Model XL-30 scanning electron microscope (SEM) with energy-dispersive X-ray microanalysis. The mean pore diameter, specific surface area and pore volume were determined by Brunauer–Emmett–Teller (nitrogen sorption isotherm) methods, using a Micrometrics particle size analyzer (model ASAP 2000). Total pore volume was calculated using the equation reported by Altenore et al. [23]. The electrokinetic properties of pumice and modified pumice were determined by a Zeta Meter 3.0 (Malvern Instruments Ltd.) equipped with a microprocessor unit. The zeta potential was calculated automatically using the Smoluchowski equation and as function of pH of the solution according to the electrophoresis method with high sensitivity. Then 0.5 g of each samples (SMP_2 and raw pumice) tasted in the zeta potential examination [24]. The pumice sample was further characterized by X-ray diffraction (XRD) and X-ray fluorescence (Philips, Model X PER MPD).

2.2. Preparation of surfactant-modified pumice (SMP)

It has been shown that chemical conditioning improved the performance of natural zeolite and sodium-type natural clinoptilolite favours the exchange of cations [25]. Therefore, the raw pumice was first pre-treated with Na^+ salt with the aim of removing certain cations from the structure and locating more easily removable ones, prior to any ion exchange applications. After conditioning, the final homoionic or near homoionic state pumice improves the effective exchange capacity. The pumice was first conditioned with 1 M NaCl solution at room temperature, and afterwards washed with distilled water and dried out at 80 °C. A pre-weighted quantity of pumice (Na-saturated) was mixed with the specified amount of hexadecyltrimethyl ammonium bromide (HDTMA) in 1 L of distilled water. The suspension was shaken for 8 h at 150 rpm and 60 °C. The solution was filtered, and then the pumice was washed several times with double distilled water, dried at 70 °C for 8 h, and used as synthetic modified pumice throughout this study. The HDTMA concentrations, which were used for pumice modification, were 0.5, 1, 2 and 3 mmol L^{-1}. The modified pumice was named $SMP_{0.5}$ (for 0.5 mmol L^{-1} surfactant), SMP_1 (for 1 mmol L^{-1} surfactant), SMP_2 (for 2 mmol L^{-1} surfactant), and SMP_3 (for 3 mmol L^{-1} surfactant). In order to evaluate isotherms of surfactant adsorption on pumice, the synthesized pumice was weighed accurately and added with the 1000 mL of HDTMA solutions in the concentration from 0.5 to 7 mmol L^{-1}. The HDTMA solutions were stirred for 24 h [15]. After 24 h shaking, the suspension was centrifuged and then the supernatants were filtered and the concentration of residual HDTMA was analyzed with a Shimadzu TOC-5000 analyzer.

2.3. Procedure of adsorption experiments

In this study, the adsorption tests were divided into two sections. In the first section, six experimental runs were designed to test the ability of SMP, to investigate the influence of operational conditions on fluoride adsorption, and to determine the optimum conditions that achieve minimum fluoride residual in the aqueous solution (maximum amount fluoride removal). In addition, in this part of the study, kinetic and isothermic data were analyzed. The details of the experimental runs and corresponding conditions are presented in Table 1. In the first run of batch adsorption experiments, 200 ml solution of fluoride of initial concentration 10 mg L^{-1} was contacted with 0.1 g of unmodified and modified pumice, separately. The contents were placed in a thermostated shaker and gently agitated at 200 rpm. The solution was filtered, and then residual the fluoride concentration was analyzed. The effects of adsorbent mass, initial pH, contact time and equilibrium test were tested in a second run of experiments (Table 1). Equilibrium adsorption was determined by mixing 0.1 g of pumice with 200 ml solution with a different concentration of fluoride (see Table 1). The amount of adsorbed fluoride at equilibrium, q_e, and fluoride removal efficiency (RE) was calculated from the mass balance equation presented in Eqs. (1) and (2), respectively.

$$q_e = \frac{V}{M} \times (C_0 - C_e) \quad (1)$$

Table 1
Experimental phases and conditions.

Experimental conditions					
Run	Purpose of experiment	Solution pH	Fluorides concentration ($mg\,L^{-1}$)	SMP ($g\,L^{-1}$)	Contact time (min)
1	Effect of HDTMA loading	6	10	0.5	20
2	Effect of pH of water	3–10	10	0.5	30
3	Effect of SMP dosage	6	10	0.15–2.5	30
4	Adsorption kinetic and effect of contact time	6	10	0.5	5–60
5	Equilibrium tests	6	1.5–20	0.5	1440
6	Effect of temperature (293–303 K)	6	10	0.5	30

$$\mathrm{RE} = \frac{C_0 - C}{C_0} \times 100 \quad (2)$$

where C_e and C_0 are the equilibrium and initial concentrations of fluoride ($mg\,L^{-1}$), respectively; q_e is equilibrium fluoride concentration on adsorbent ($mg\,g^{-1}$); V is the volume of fluoride solution (L); M is the mass of SMP sample used (g); and RE is the removal efficiency. Apart from the correlation coefficient (R^2), the validity of the adsorption isotherm and its goodness-of-fit was evaluated with Marquardt's percent standard deviation (MPSD) and the hybrid error function (HYBRID), which can be described as:

$$\mathrm{MPSD} = 100\sqrt{\frac{1}{N-P}\sum_{i=1}^{N}\left(\frac{q_{ei}^{\exp} - q_{ei}^{\mathrm{cal}}}{q_{ei}^{\exp}}\right)^2} \quad (3)$$

$$\mathrm{HYBRID} = \frac{100}{N-P}\sum_{i=1}^{N}\left[\frac{(q_{ei}^{\exp} - q_{ei}^{\mathrm{cal}})^2}{q_{ei}^{\exp}}\right] \quad (4)$$

where $q_{ei}^{\exp}$ is the observation from the batch experiment i; q_{ei}^{cal} is estimated from the isotherm for the corresponding $q_{ei}^{\exp}$; N is the number of observations in the experimental isotherm; and P is the number of parameters in the regression model. The smaller MPSD and HYBRID values reveal more accurate estimations of q_e values [26,27]. In addition, in kinetics studies, apart from the correlation coefficient (R^2), the validity of kinetic models has been measured by the normalized standard deviation (NSD) and average relative error (ARE), which can be defined as:

$$\mathrm{NSD} = 100\sqrt{\frac{1}{N-1}\sum_{i=1}^{N}\left[\frac{(q_t^{\exp} - q_t^{\mathrm{cal}})}{q_t^{\exp}}\right]^2} \quad (5)$$

$$\mathrm{ARE} = \frac{100}{N}\sum_{i=1}^{N}\left|\frac{q_e^{\exp} - q_e^{\mathrm{cal}}}{q_e^{\exp}}\right|_i \quad (6)$$

where $q_t^{\exp}$ and q_t^{cal} ($mg\,g^{-1}$) are experimental and calculated fluoride adsorbed on SMP at time t, and N is the number of measurements made. The smaller NSD and ARE values indicate more accurate estimations of q_t values [27].

In the second section of this work, the applicability of SMP in the removal of fluoride from natural water was examined. The water samples were collected from the city of Bahar in the west of Iran. The water quality parameters of samples were determined before and after of treatment by SMP. The water qualities of collected samples were analyzed using standard methods [28].

2.4. Fluoride analysis and chemicals

The fluoride concentration in the solutions was determined by expandable ion analyses (Orion EA 940 ion meter) [28]. The pH was measured via the EA 940 ion meter with a pH electrode. NaF and hexadecyltrimethyl ammonium bromide (HDTMA) were obtained from Merck Co. All chemicals were reagent grade and used without further purification. All experiments were conducted in duplicate, and the average values are presented.

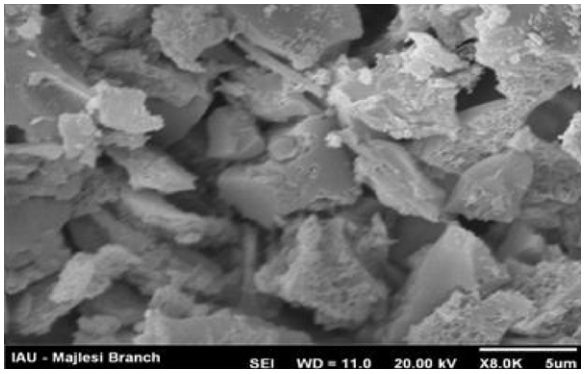

Fig. 1. Scanning electron micrograph (SEM) image of natural particle.

3. Results and discussion

3.1. Pumice characterization

SEM was used to observe the natural and modified pumice morphology, and micrographs are shown in Figs. 1 and 2. The image of the original pumice (Fig. 1) indicated that the pumice surface had a porous surface. The SEM modified pumice (SMP_2) is given in Fig. 2. As seen in Fig. 2, the surfaces of original pumice clearly changed after modification, and porous surface could not be seen clearly. The reason is that the external surface of pumice was covered by surfactant (Fig. 2). In other words, the HDTMA was adsorbed on the external surface of the pumice. The results of X-ray diffraction (XRD) spectra (Fig. 3) demonstrated that the main component of pumice was SiO_2, with the largest intensity peaks related to SiO_2 (quartz). From the X-ray fluorescence (XRF) results, pumice is composed of SiO_2 (65.219%), Al_2O_3 (15.5%), CaO (2.508%), MgO (0.862%), Na_2O (1.814%), K_2O (2.681%) and Fe_2O_3 (2.606%). Approximately 8.07% of the pumice sample was lost in

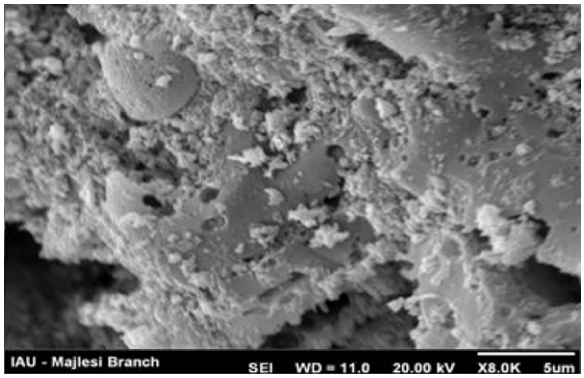

Fig. 2. Scanning electron micrograph (SEM) image of SMP_2.

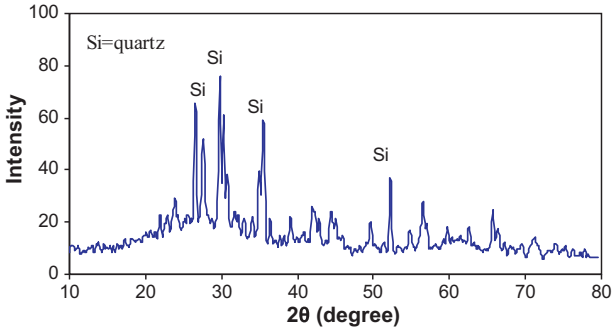

Fig. 3. XRD pattern of pumice.

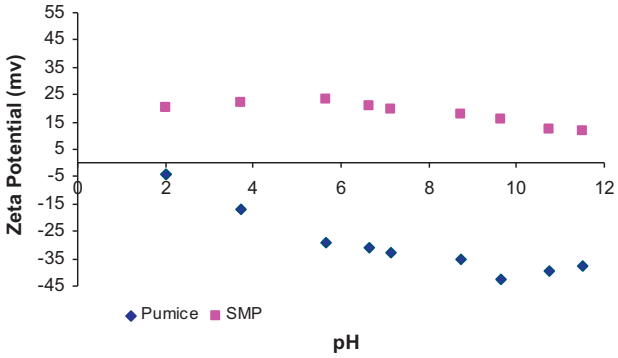

Fig. 4. Zeta potential vs. pH of the natural and modified pumice (SMP_2).

the ignition process. Various studies have reported that the main component of pumice is SiO_2 [22,29]. The BET-specific surface area, total pore volume and mean pore diameter (at $P/P = 0.99$) of the unmodified and modified pumice were determined using the BET isotherm model. The specific surface area, total pore volume, and mean pore diameter of the natural pumice were 13.77 $m^2\,g^{-1}$, 0.0052 $cm^3\,g^{-1}$ and 15.297 nm, respectively. The ratios of SiO_2 to Al_2O_3 and BET of selected pumice in this study are smaller than other sources regarding pumice [22,29]. The geological formation of pumice sources can probably attribute to differences in the compound and BET of pumice. In addition, the specific surface area, total pore volume, and mean pore diameter of the modified pumice were 11.79 $m^2\,g^{-1}$, 0.0041 $cm^3\,g^{-1}$ and 23.2 nm, respectively. The specific surface area and pore volume of the natural pumice decreased, as it was modified with surfactant. Due to modification, some of the main channels of the pumice became obstructed by surfactant; therefore, the diffusion of N_2 into these channels was impeded, and resulted in decreasing the specific surface area and pore volume. The mean pore diameter of the natural pumice after modification was increased, perhaps the result of the blockage of the smallest pore diameters with surfactant; and consequently, the mean pore diameter increased.

3.2. Effect of the modifier loading level and maximum adsorption of HDTMA onto pumice

In Run 1 experiments, the effect of HDTMA loading levels on fluoride adsorption was conducted in a range of 0.5–3 mmol L^{-1}. The experimental results indicated that 55–98% of HDTMA adsorbed on pumice. The results show that treatment with initial concentration of 2 mmol L^{-1} of HDTMA, adsorbed about 92% of fluoride onto pumice and appeared to be the optimal loading for fluoride removal. The results of the application of modified and original pumice on fluoride removal are presented in Table 2. Table 2 reveals that the level of adsorbed fluoride onto natural pumice is very little (12%). The zeta potential profiles of natural and modified pumice vs. pH are given in Fig. 4. As seen in Fig. 4, raw pumice has a negative charge in the entire pH range. Ersoy et al. [30] also reported that pumice has a negative charge. Since the fluoride ion has negative charge, it is repelled by the negatively charged pumice surface. This induces a relatively low adsorption capacity, as shown in Table 2. For this reason, in order to increase the adsorption capacity, the surface of natural pumice was modified with a typical HDTMA, which neutralizes the negative charges. The results in Fig. 4 indicated that the surface acquires positive charges and consequently become receptive to the uptake of negatively charged fluoride ion through electrostatic attraction. No information could be found in literature on the zeta potential of the modified pumice by HDTMA to compare with our results. However, Armagan et al. [24] reported that negative surface charge of natural zeolite changed to positive after modification with HDTMA. Schematic diagram of HDTMA configurations on the pumice surface and fluoride adsorption onto SMP are given in Fig. 5. At low concentration, HDTMA forms a monolayer on the pumice surface with the hydrophobic ends of the molecules reaching out in the solution (Fig. 5a). At low surfactant concentration there will be no adsorption of fluoride ion due to hydrophobic surface. With increasing coverage, also a second HDTMA layer may be formed. This bilayer presents positively charged functional groups towards the solution, which can serve as sorption sites for anions (Fig. 5b). As seen in Fig. 5, the formation of bilayer at 2 mmol L^{-1} concentration of HDTMA on pumice surface, there by protruding cationic head group towards water for chemisorptions with fluoride ion (Fig. 5b). This result shows that original pumice is not an appropriate adsorbent for fluoride elimination from water. However, in the SMP, the percent of fluoride removal increased as HDTMA levels increased to 2 mmol L^{-1}, and this level of modifier led to the maximum removal of fluoride (92.5%) at 20 min contact time. Therefore, it is concluded that modification with an initial concentration of 2 mmol L^{-1} of HDTMA

Table 2
Comparison of fluoride removal efficiency of natural and modified pumice.

	Type of pumice				
	Raw pumice	$SMP_{0.5}$	SMP_1	SMP_2	SMP_3
Removal efficiency (%)	12	70	80	92.5	87

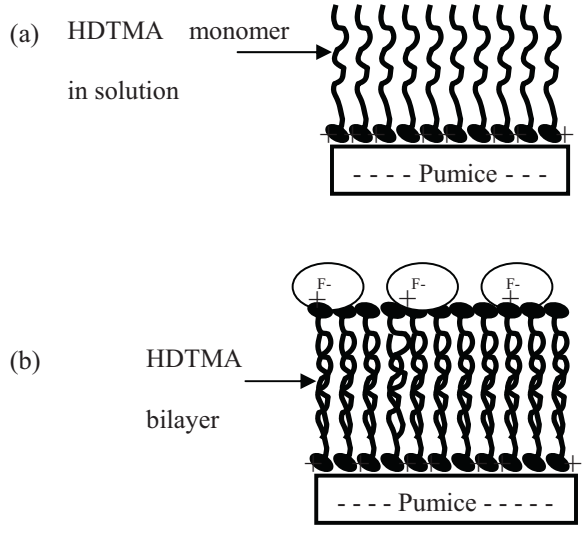

Fig. 5. Schematic diagram of the theoretical monolayer and bilayer of HDTMA formation on the pumice structure (a and b), and interaction of fluoride ion with HDTMA on pumice surface (b).

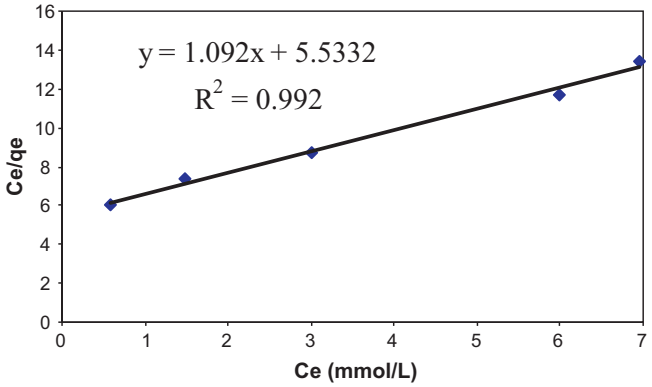

Fig. 6. Adsorption isotherm of HDTMA onto Na-pumice.

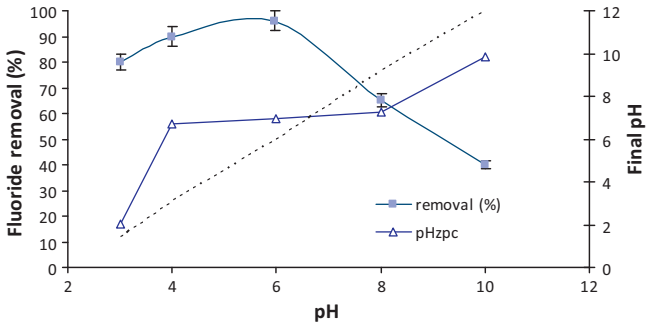

Fig. 7. Effect of pH on fluoride adsorption and pH_{zpc} draft.

gives the best performance, and thus it was selected as an optimal loading level for fluoride removal and used for the rest of the experiments. Furthermore, an increase of surfactant concentration up to 3 mmol L^{-1} resulted in a decline of fluoride removal efficiency (87%). An increase in adsorption with an HDTMA loading value ranging from 0.5 to 2 mmol L^{-1} can be explained by changes in pumice surface charge due to modification with HDTMA. When the pumice is treated with HDTMA, due to the increase of positive charges on the surface of pumice, electrostatic forces between the positive charges on the surface of pumice and fluoride in the solution increased that enhances fluoride removal [31].

Results from experimental of sorption of HDTMA from solution onto surfaces pumice indicated that adsorption of HDTMA on pumice could be best followed with the Langmuir isotherm (Fig. 6 and Table 3). The sorption isotherm for HDTMA on the Na-pumice is presented in Fig. 6. When fitting the data (Fig. 6) into Eq. (15) in Section 3.6, it was found that the high coefficient of determination (R^2) as shown in Fig. 6, indicating good agreement with Langmuir model. The maximum of the HDTMA adsorbed onto pumice (Q_{max}) can be calculated from the equation given in Fig. 6 and was showed in Table 3. Wingenfelder et al. [15] and Rozic et al. [32] have also obtained a better fit using the Langmuir isotherm for experimental data for HDTMA adsorption onto zeolite. The maximum moles of HDTMA adsorbed on the SMP were 0.916 mmol g^{-1}. It can be suggested that the HDTMA molecule may create an organic-rich layer on the pumice surface and the charge on the surface is reversed from negative to positive.

3.3. Effect of solution pH

Since the pH of the aqueous solution plays a key role in the adsorption process, in Run 2 experiments, the effect of solution pH on the removal of fluoride by SMP was examined in a range of 3–10 under the conditions presented in Table 1. The results of pH effect on fluoride removal are shown in Fig. 7. This figure clearly shows that the adsorption of fluoride was highly affected by the solution pH. Similar observations were reported for fluoride adsorption onto modified activated carbon and hydroxyapatite by other authors [33,34]. As seen from the figure, under acidic and alkaline conditions, the lowest amounts of fluoride were removed. Fig. 7 also demonstrates that fluoride adsorption in SMP decreased from 96% to 40% when the pH solution increased from 6 to 10.

Table 3
Fitted Langmuir parameters for sorption of HDTMA by pumice.

Slope ($1/Q_{max}$)	Intercept ($1/bQ_{max}$)	Q_{max} (mmol g^{-1})	b (g^{-1})	R^2
1.092	5.5332	0.916	0.197	0.992

Fluoride-contaminated groundwater contains several other ions that can compete with fluoride in the adsorption process. The decrease in fluoride removal under alkaline conditions may be due to competition of excess of hydroxyl ions with fluoride ions for active sites on SMP. This finding agrees with other researchers who have also reported that hydroxyl ions, bicarbonate, carbonate, chloride, sulfate and nitrate have negative effects on fluoride adsorption by modified chitosan [34,35]. In addition, the trend in fluoride removal in the presence of coexisting anions seems to be related to the valence of the coexisting anions. Trivalent ions have the largest effect while monovalent anions give the least effect [34,35]. This trend supports the conclusion that electrostatic interaction plays a major role in fluoride uptake by SMP.

The decrease in fluoride removal under alkaline conditions can also be described by considering the point of zero charge (PZC) of the SMP and the nature of fluoride (negative charge of fluoride ions). Fig. 7 also shows the plot of equilibrium pH (final pH) against the initial pH. As seen from the figure, the PZC value of SMP particles' surface was 6.5. This means that the SMP surface was negatively charged at solution pHs above 6.5, and fluoride ions were repelled by the SMP surface, resulting in the reduction of fluoride adsorption [13]. However, at pH values below the PZC (pH_{zpc} = 6.5) of SMP, the surface of SMP was positively charged, causing better fluoride ions adsorption through the electrostatic attraction. Up to now, there was no previous report on fluoride adsorption by SMP. However, Ramos et al., Anirudhan and Ramachandran evaluated the influence of pH on chromium and acid humic adsorption by surfactant-modified zeolite (SMZ) and surfactant-modified bentonite (SMB), respectively [13,36]. These authors evaluated the adsorption of chromium and acid humic from an aqueous solution on SMZ and SMB at different pHs and found that the surfactant modified zeolite surface was negatively charged at pH > PZC and due to their negative charge, anions were repelled by the SMZ surface [13,36]. In addition, the lower amount of fluoride removed under acidic conditions (pH 3–5) may be due to the formation of weak hydrofluoric acid. As seen in Fig. 7, the highest fluoride ions uptake of 96% was observed at pH 6. Therefore, the optimum pH was 6, and the rest of the examinations were evaluated at this optimum pH. As shown in Table 4, our findings are in agreement with only some results reported previously about fluoride adsorption [37–42]. This study's results may be different from others due to the use of different adsorbents and operational conditions.

3.4. Effect of SMP dosage

The effect of SMP dosage on fluoride adsorption was studied in the range of 0.15–2.5 g L^{-1} in Run 3 experiments under the conditions specified in Table 1. The results regarding fluoride removal and adsorption capacity at various SMP doses are presented in Fig. 8. According to Fig. 5, increasing the SMP dosage from 0.15 to 0.5 g L^{-1} also increases percentage fluoride removal from 80% to

Table 4
Comparison of fluoride adsorption capacity using SMP with different adsorbent.

Adsorbent	Optimum pH	Fitted kinetic model	Fitted isotherm model	Adsorption capacity (mg g^{-1})	Reference
Ceramic	7	Pseudo-second-order	Freundlich and Langmuir	2.16	37
Hydrous iron(III)–tin(IV) bimetal	3	Pseudo-second-order	Langmuir	10	38
Nano-hyrdroxyapatite/chitin	3	Pseudo-second-order	Langmuir	8.4	39
Ferric hydroxide	7	Pseudo-second-order	Langmuir	6.5	40
Nano-alumina	6.15	Pseudo-second-order	Langmuir	14	41
CaO/activated alumina	5.5	Pseudo-second-order	Langmuir	101.01	42
MnO_2/activated alumina	5.5	Pseudo-second-order	Langmuir	10.18	42
Activated alumina	5.5	Pseudo-second-order	Langmuir	24.39	42
SMP	6	Pseudo-second-order	Langmuir	41	This study

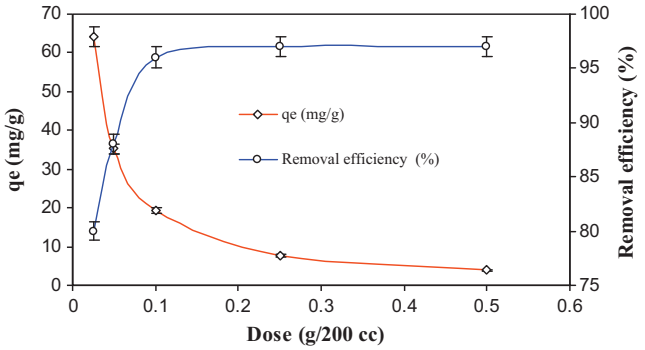

Fig. 8. Effect of SPM dose for fluoride adsorption.

97% after 30 min contact time; an equilibrium value was reached after 0.5 g L^{-1} of sorbent dosage. The enhancement of fluoride adsorption as a function of SMP dose to 0.5 g L^{-1} is due to the greater availability of active binding sites and to the presence of a greater surface area for adsorption. In addition, it can be seen that the rate of fluoride adsorbed to SMP (mg g^{-1}) did not significantly increase with the increasing dosage of SMP from 0.5 to 2.5 g L^{-1}. One plausible reason could be due to overlap of active sites at higher adsorbent masses resulting in reduced effective surface area required for sorption [31]. In addition, when the SMP dosage increased from 0.5 to 2.5 g L^{-1}, the percentage of fluoride removal exhibited no significant increase. Thus, 0.5 g L^{-1} of SMP was fixed as the optimum dosage, and the rest of the studies were performed at this optimum adsorbent dose.

3.5. Kinetics of fluoride adsorption on SMP

In Run 4 experiments, the effect of contact time in the range of 5–60 min and kinetics were evaluated under conditions shown in Table 1. Fig. 9 illustrates the time profile of fluoride adsorption onto modified pumice in terms of removal efficiency and adsorption capacity. As shown in this figure, as contact time increased, adsorption capacity of fluoride and removal efficiency increased,

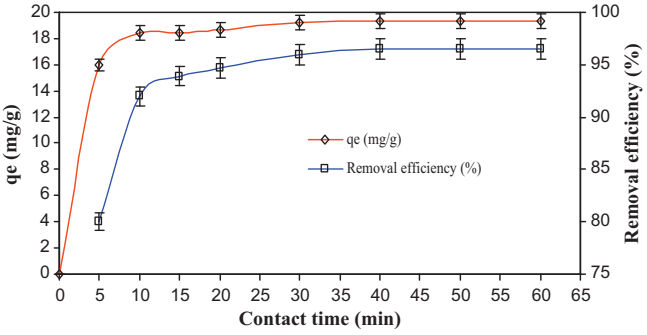

Fig. 9. Influence of contact time on adsorption of fluoride by SMP.

but then gradually reached equilibrium after 30 min contact time. Hence, 30 min contact time was selected as the optimum time for the sorbents for further examination. The kinetic adsorption data are probably the most important factor in the design of an adsorption system, to determine the adsorbate uptake rate and the time needed to attain equilibrium for industrial applications [33,43]. To analyze the kinetics of adsorption onto SMP, two simplified kinetics models including the pseudo first-order Lagergren and pseudo-second order were used. The pseudo first-order model is generally given by [33,43–45].

$$\frac{dq_t}{d_t} = k_1(q_e - q_t) \tag{7}$$

where k_1 is the pseudo first-order rate constant (min^{-1}), and q_e and q_t are the adsorption capacity at equilibrium conditions (mg fluoride/g SMP) and at time t, respectively. After integrating Eq. (7) between the limits, $t = 0$ to $t = t$ and $q_t = 0$ to $q_t = q_e$, we obtain:

$$\log(q_e - q_t) = \log(q_e) - \frac{k_1}{2.203}t \tag{8}$$

In addition, the non-linear form of the pseudo second-order equation is expressed as

$$\frac{dq_t}{d_t} = k_2(q_e - q_t)^2 \tag{9}$$

where k_2 is the rate of the pseudo second order model (g mg^{-1} min^{-1}). Eq. (9) can be linearized onto at least four different forms (Eqs. (10)–(13)).

$$\text{Type 1}: \quad \frac{t}{q_t} = \frac{1}{k_2 q_e^2} + \frac{t}{q_e} \tag{10}$$

$$\text{Type 2}: \quad \frac{1}{q_t} = \left(\frac{1}{k_2 q_e^2}\right)\left(\frac{1}{t}\right) + \left(\frac{1}{q_e}\right) \tag{11}$$

$$\text{Type 3}: \quad q_t = q_e - \left(\frac{1}{k_2 q_e}\right)\frac{q_t}{t} \tag{12}$$

$$\text{Type 4}: \quad \frac{q_t}{t} = k_2 q_e^2 - k_2 q_e q_t \tag{13}$$

The parameters in these models (first and second order) can be determined experimentally from plotting $\log(q_e - q_t)$ vs. t, (t/q_t) vs. t, $1/q_t$ vs. $1/t$, q_t vs. q_t/t and q_t/t vs. q_t, respectively [27,44]. The values of correlation coefficients NSD and ARE from the fitted kinetic models are presented in Table 5. The fitted linear regression plots showed that the experimental data are well fitted to the pseudo-second-order kinetic model type1 with higher value correlation coefficient ($R^2 > 0.999$), compared to pseudo-second-order kinetic model types 2, 3, 4 and the pseudo-first-order model. The fitted kinetic models were further evaluated by determining the NSD, ARE and adsorption capacities. As shown in Table 5, NSD and ARE for pseudo-second-order kinetic model type1 were 7.67% and 6.47%, respectively. The comparison of the NSD and ARE values in Table 4 confirm that fluoride adsorption onto SMP fits well with pseudo-second order kinetic model type 1, validating

Table 5
Values of the pseudo first and second order parameters for fluoride sorption onto SMP.

Information	Pseudo-first order	Pseudo-second order (Type 1)	Pseudo-second order (Type 2)	Pseudo-second order (Type 3)	Pseudo-second order (Type 4)
R^2	0.975	0.999	0.972	0.973	0.972
NSD	20	7.67	9.67	15.67	14.67
ARE	12	6.45	8.45	12.45	11.45

this model for the adsorption of fluoride onto SMP (see Fig. 10). Moreover, the results, based on this model (as seen in the inset of Fig. 10) indicate that two reactions in either series or in parallel are completed in the adsorption of fluoride by SMP; the first one is fast and the second is a slower reaction that can continue for a long period of time. In addition, the fitness of experimental data to the pseudo-second order model, the basic assumption in the model, implies that chemisorption plays a major role and likely controls the adsorption process [44]. From the correlation coefficient, NSD and ARE values, the best kinetic model fitted the data in the following order:

Pseudo-second-order (type 1) > pseudo-second-order (type 2) > pseudo-second-order (type 4) > pseudo-second-order (type3) > pseudo-first-order

The fitted linear form of the pseudo-second order model is shown in Fig. 10. The results in Fig. 10 show that the fitted model with data was $t/q_t = 0.033 + 0.0511t$, and the model-calculated adsorption capacity ($q_{e,cal}$) was 19.3 mg g^{-1}. Fig. 10 also reveals that the value calculated from the model ($q_{e,cal}$) was very close to the experimental adsorption capacity value ($q_{e,exp}$ = 19.15 mg g^{-1}). These data strongly suggest that the pseudo-second order kinetic model provides a good correlation for the adsorption fluoride on SMP. These findings are in agreement with most previous studies examining the adsorption of fluoride onto different adsorbents, as indicated in Table 4.

3.6. Equilibrium adsorption isotherms

Isotherms express the specific relationship between the amount of fluoride adsorbed onto SPM surface in given experimental conditions and the equilibrium concentration of fluoride in the liquid phase. Therefore, an analysis of isotherm data was conducted to determine the maximum capacity of the sorbent and to develop an equation for the purpose of a column design. Accordingly, the conformity experimental results with four of the most conventional isotherm models Langmuir (four types), Freundlich, Dubinin–Radushkuvich and Temkin were evaluated in Run 5 experiments. The coefficient (R^2), MPSD and HYBRID were used to select the best-fit isotherm model. The linear form of the selected models can be represented by the following equations [27,33,44,45]:

$$\text{Freundlich}: \quad \ln q_e = \ln k_f + \frac{1}{n}\ln C_e \tag{14}$$

$$\text{Langmuir-1}: \quad \frac{C_e}{q_e} = \frac{1}{bQ_{max}} + \frac{C_e}{Q_{max}} \tag{15}$$

$$\text{Langmuir-2}: \quad \frac{1}{q_e} = \left(\frac{1}{Q_{max}b}\right)\frac{1}{C_e} + \frac{1}{Q_{max}} \tag{16}$$

$$\text{Langmuir-3}: \quad q_e = Q_{max} - \left(\frac{1}{b}\right)\frac{q_e}{C_e} \tag{17}$$

$$\text{Langmuir-4}: \quad \frac{q_e}{C_e} = bQ_{max} - bq_e \tag{18}$$

$$\text{Temkin}: \quad q_e = B_T \ln A_T + B_T \ln C_e \tag{19}$$

$$\text{Dubinin–Radushkevich(D-R)}: \quad \ln q_e = \ln Q_{max} - K_{DR}\varepsilon^2 \tag{20}$$

In 1906, the Freundlich presented the earliest known sorption isotherm equation. In this study, the Freundlich was selected to estimate the adsorption intensity of the fluoride ion on the SMP surface based on sorption heterogeneous energetic distribution of active sites attended by interactions between adsorbed molecules [45]. The Freundlich model is an empirical method for adsorbents with heterogeneous adsorbing surfaces (Eq. (14)); q_e and C_e in Eq. (14) are parameters that are described in Eqs. (1) and (2); k_F and $1/n$ are constants that depict the adsorption capacity and the adsorption intensity, respectively; and k_F and n can be determined by a plot of q_e vs. $\ln C_e$. The results from the isotherm evaluation are given in Table 6. As shown in Table 5, based on the reported correlation coefficients, MPSD and HYBRID, the Freundlich model is less applicable to SMP than the Langmuir isotherms. The Langmuir adsorption model is takes the best-known theoretical treatments of non-linear sorption and suggests that adsorption take place on a homogeneous surface by monolayer sorption without interaction between adsorbent molecules. Besides, the model assumes uniform energies of adsorption onto the surface [44,45]. Therefore, the Langmuir isotherms were chosen to determine the maximum adsorption capacity corresponding to the complete monolayer coverage on the SMP. In this study, four forms of the linear model of Langmuir were evaluated to conform to experimental data obtained in the study (Eqs. (15)–(20)).

In the Langmuir equations (Eqs. (15)–(20)), Q_{max} (mg g^{-1}) and b are constant and can be determined from the slope and intercept. Q_{max} is the maximum amount of adsorption fluoride at complete monolayer coverage (mgF/gSMP), and b (L mg^{-1}) is the adsorption equilibrium constant [33].

Based on the coefficient of correlation, the Langmuir model (type 1) was best fitted to the experimental data. In addition, based on the information in Table 6, the MPSD (4.11%) and HYBRID (3.5%) values of the Langmuir model (type 1) were lower than those of the other evaluated models. The data show that the experimental results are best described by the Langmuir isotherm type 1 equation. Therefore, the experimental results suggest that a monolayer of fluoride ions is adsorbed on homogeneous adsorption sites on the surface of SMP. As shown in Table 4, these data conform to the findings of previously studies that employed the Langmuir model to explain the adsorption of fluoride onto different adsorbents.

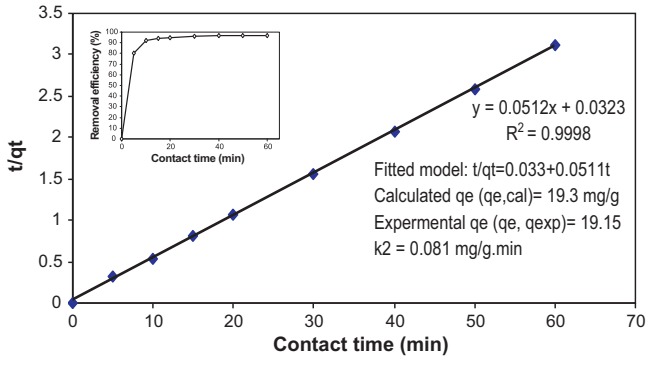

Fig. 10. Pseudo-second-order sorption of fluoride adsorption onto SMP.

Table 6
Summary of equilibrium isotherm parameters.

Isotherms	R^2	MPSD	HYBRID	Information
Freundlich model	0.95	18	12	$n = 3.2$ $K_F = 27.6$
Langmuir model, Type (1)	0.999	4.11	3.5	$Q_{max} = 41.65$, $b = 0.249$ $R_L = 0.167$
Langmuir model, Type (2)	0.988	8.7	6.8	$Q_{max} = 39.21$, $b = 0.255$ $R_L = 0.163$
Langmuir model, Type (3)	0.987	12.4	9.7	$Q_{max} = 41$, $b = 0.247$ $R_L = 0.168$
Langmuir model, Type (4)	0.989	10.5	7.8	$Q_{max} = 41.145$, $b = 0.247$ $R_L = 0.168$
Temkin	0.952	12	16	$Q_{max} = 32.46$, $A_T = 1.618$
Dubinin-Radushkevich	0.89	18	21	$Q_{max} = 5.7$, $K_{DR} = 0.0021$

As seen in Table 6, the best fit adsorption isotherms for the sorption of fluoride on SMP can be listed in the following order:

Langmuir-1 > Langmuir-4 > Langmuir-2 > Langmuir-3 > Temkin > Freundlich > Dubinin–Radushkevich

The essential feature of the Langmuir isotherm can be described with a dimensionless separation factor or equilibrium constant R_L, which is used for the description of the adsorption condition, expressed as [29]: $R_L = 1/(1 + bC_0)$. The value of R_L represents the adsorption situations to be either unfavorable ($R_L > 1$), linear ($R_L = 1$), favorable ($R_L < 1$), or irreversible ($R_L = 0$) [27,33]. Based on the Langmuir constant, the value of this parameter ($R_L = 0.167$) for fluoride adsorption with SMP falls between 0 and 1, which confirms that fluoride adsorption with this adsorbent is favorable under the conditions of this research (Table 6). In addition, the n value, a constant of the Freundlich model (3.2), is greater than 1, which indicates that SMP is an appropriate adsorbent and beneficial for the adsorption of fluoride from water. A comparison of absorption capacities of some adsorbents has been made between SMP in this study and previously reported for fluoride removal (see Table 4). Referring to Table 4, the Q_{max} (mg g^{-1}) of SMP for adsorbing fluoride was 41 mg g^{-1}. Clearly, from the information gathered in Table 4, SMP examined in this study demonstrates the highest adsorption capacity in comparison to most other adsorbents in terms of defluoridation capacity. The Temkin model described the effects of some indirect adsorbate–adsorbate interaction on adsorption isotherms. This model demonstrated that the heat of adsorption of all the molecules on adsorbent surface layer would decrease linearly with coverage due to adsorbate–adsorbate interactions. Then, the adsorption capability of the adsorbent for adsorbates can be assessed using Temkin model, which assumes that the fall in the heat of sorption is linear rather than logarithmic, as denoted in the Freundlich model [44,45]. The Temkin isotherm is represented by the following equation:

$$q_e = \frac{RT}{b}\ln(A_T C_e) \tag{21}$$

The linear form of this equation is shown in Eq. (19). In the Temkin model, A_T (L g^{-1}) is the binding constant that represents the maximum binding energy, $B_T = (RT)/b$ is the Temkin constant, R is the universal gas constant, 8.314 J mol K^{-1}, and T is the absolute temperature in Kelvin. The constant b is related to the heat of adsorption [45]. For the analysis of data with the Temkin model, the parameters of the equation have been determined with a plot of q_e vs. $\ln C_e$.

Table 6 depicts further that the experimental data had also a good correlation with the Temkin isotherm ($R^2 = 0.952$). The Temkin adsorption potential ($B_T \ln A_T$) of SMP is 15.63 kJ mol^{-1} that it is greater than 8 kJ mol^{-1}, illustrating that the bond between fluoride ions and the SMP surface is very strong [46].

Since Langmuir and Freundlich isotherms do not give information about mechanisms and the energy needed for adsorption, other isotherms should be used to determine the adsorption mechanism and energy required for the process. This information can be obtained using the Dubinin–Radushkevich (D-R) isotherm (Eq. (20)). Isotherm does not assume a homogeneous surface or a constant sorption potential. In the D-R model, ε (Polanyi potential) is $RT\ln(1 + 1/C_e)$, Q_{max} is the adsorption capacity(mg g^{-1}), K_{DR} is a constant related to adsorption energy, and R and T are the gas constant and temperature (K), respectively [44,45]. The value of K_{DR} (mol^2 (kJ^2)$^{-1}$) can be calculated from the slope of the plot of $\ln q_e$ vs. ε^2, and Q_{max} (mg g^{-1}) is determined from the intercept. As mentioned above, K_{DR} is related to energy adsorption, so the mean free energy of adsorption (E) can be calculated from the K_{DR} value using the following equation:

$$E = \frac{1}{\sqrt{2K_{DR}}} \tag{22}$$

Based on the D-R isotherm in Table 6, the calculated value of E as free energy of adsorption is 15.5 kJ mol^{-1}. The amount of E between 8 and 16 kJ mol^{-1} demonstrates that chemical adsorption plays a significant role under the operation conditions [45]; accordingly, the adsorption of fluoride by SMP appears by a mechanism of chemisorptions, which is in agreement with the information obtained from kinetic evaluation.

These data indicate that the SMP has a high adsorption capacity, and pumice is abundantly available at very low costs. These characteristics, along with the simplicity of its use and operation, confirm that SMP is a promising, efficient, and economic adsorbent for fluoride removal from water.

3.7. Thermodynamic investigations of fluoride adsorption onto SMP

In order to explain and confirm the mechanism of fluoride adsorption onto SMP, the thermodynamics parameters of adsorption under the conditions specified in Table 1 were evaluated using standard free energy change (ΔG°), standard enthalpy change (ΔH°),and standard entropy change (ΔS°) and sticking probability (SP^*), given by Eqs. (23)–(25).

$$\Delta G^\circ = -RT\ln K_\circ \tag{23}$$

$$\ln K_\circ = -\frac{\Delta H^\circ}{RT} + \frac{\Delta S^\circ}{R} \tag{24}$$

$$SP^* = (1-\beta)\exp -\left(\frac{E_a}{RT}\right) \tag{25}$$

where β is surface coverage. The plot of $\ln(1-\beta)$ against $1/T$ will give a linear plot with intercept of $\ln SP^*$ and slope of E_a/R. The values of ΔH° and ΔS° can be obtained from the slope and intercept of a plot of $\ln K$ against $1/T$. As seen in Table 7, the value of ΔG° for all tested temperatures was calculated to be negative, which suggests that the adsorption of fluoride onto SMP is spontaneous and

Table 7
Thermodynamic parameter of fluoride adsorption onto SMP.

Parameter	Temperature (K)	SMP
	293	−2.5
ΔG° (kJ mol^{-1})	298	−2.63
	303	−2.92
ΔS° (kJ (mol K)$^{-1}$)		0.0232
ΔH° (kJ mol^{-1})		4.422
SP*		0.001

Table 8
Characteristics of actual drinking water quality before and after adsorption.

Water quality	Concentration before treatment (mg L^{-1})	Concentration after treatment (mg L^{-1})
F^-	5	0.5
Cl^-	23	15
Na^+	9.6	9.2
K^+	0.4	0.3
NO_3^-	8	2
SO_4^-	15	12
TH	198	195
TDS	186	174

indicates that SMP has a high affinity for the adsorption of fluoride from solution under experimental conditions [33].

Furthermore, the values of ΔH° and ΔS° in the present experiment were 4.422 kJ mol^{-1} and 0.0232 kJ (mol K)$^{-1}$, respectively. A positive value of ΔH° proves the adsorption phenomenon is endothermic [33,47]. Furthermore, the positive value of ΔS° indicates increased randomness at the interface of SMP solution during the adsorption process [33,47]. The value of SP* which was very close to zero confirmed the dominance of chemisorption mechanism [33]; thus, the results of thermodynamic investigation reconfirmed the hypothesis of chemisorption of fluoride onto SMP.

3.8. Application of SMP to fluoride removal from drinking water

The ability of SMP in field conditions was tested with water samples collected from the city of Bahar in the west of Iran in the second section of this study. Fluoride was adsorbed from 1 L of groundwater at optimum conditions, determined from Section 1 of this work. The water quality of the sample prior to and post treatment is presented in Table 8. The results depict that the residual fluoride in drinking water after treatment was 0.5 mg L^{-1} lower than the maximum allowable concentration value recommended by the WHO. The results of this study indicated that SMP is a cheap and efficient adsorbent that can be used for the elimination of excess fluoride from water.

4. Conclusion

The findings of this study revealed that functionalized original Iranian pumice caused a decrease in its surface area, due to pore blocking. The adsorption process is pH dependent, and the optimum pH was 6. The kinetic studies showed that the adsorption data are fitted well to the pseudo-second order model (type 1). Furthermore, the isotherm equilibrium studies confirmed that the Langmuir-1 form is the best-fitted model for the adsorption process of fluoride by modified pumice. The maximum adsorption capacity of fluoride was 41 mg g^{-1}, and the optimal dosage of SMP was 0.5 g L^{-1}. Results from the field trial of SMP for the treatment of groundwater suggest that the maximum permissible concentration of fluoride is achievable, even when the initial fluoride concentration exceeds 1.5 mg L^{-1}. Accordingly, the SMP was shown to be an efficient adsorbent for the removal of fluoride and a promising option for water fluoride treatment. However, further studies will be required to scale up and optimize process variables.

Acknowledgements

The authors are grateful to the Hamadan University of Medical Sciences for its technical and financial support of this research.

References

[1] M. Kanbur, G. Eraslan, S. Silici, M. Karabacak, Effects of sodium fluoride exposure on some biochemical parameters in mice: evaluation of the ameliorative effect of royal jelly applications on these parameters, Food Chem. Toxicol. 47 (6) (2009) 1184–1189.
[2] M. Mohapatra, S. Anand, B.K. Mishra, D.E. Giles, P. Singh, Review of fluoride removal from drinking water, J. Environ. Manage. 91 (1) (2009) 67–77.
[3] J.L. Adam, Fluoride glass research in France: fundamentals and applications, J. Fluorine Chem. 107 (2001) 265–270.
[4] V. Khatibikamal, A. Torabian, F. Janpoor, G. Hoshyaripour, Fluoride removal from industrial wastewater using electrocoagulation and its adsorption kinetics, J. Hazard. Mater. 179 (2010) 276–280.
[5] G. Somer, S. Kalaycı, İ. Başak, Preparation of a new solid state fluoride ion selective electrode and application, Talanta 80 (2010) 1129–1132.
[6] A. Schneir, R.F. Clark, M. Kene, D. Betten, Systemic fluoride poisoning and death from inhalational exposure to sulfuryl fluoride, Clin. Toxicol. (Phila) 46 (2008) 850–854.
[7] D. Ghosh, C.R. Medhi, M.K. Purkait, Treatment of fluoride containing drinking water by electrocoagulation using monopolar and bipolar electrode connections, Chemosphere 73 (2008) 1393–1400.
[8] C. David, M.C. Herbert, 65,000 GPD fluoride removal membrane systems in Lakeland, California, USA, Desalination 117 (1998) 19–35.
[9] K. Hu, M.D. James, Nanofiltration membrane performance on fluoride removal from water, J. Membr. Sci. 279 (2006) 529–538.
[10] A. Ramdani, S. Taleb, A. Benghalem, N. Ghaffour, Removal of excess fluoride ions from Saharan brackish water by adsorption on natural materials, Desalination 250 (2010) 408–413.
[11] A. Çinarli, O. Biçer, M. Mahramanlioglu, Removal of fluoride using the adsorbents produced from mining waste, Fresenius Environ. Bull. 14 (2005) 520–525.
[12] A. Tor, N. Danaoglu, G. Arslan, Y. Cengeloglu, Removal of fluoride from water by using granular red mud: batch and column studies, J. Hazard. Mater. 164 (2009) 271–278.
[13] R. Leyva-Ramos, et al., Adsorption of chromium(VI) from an aqueous solution on a surfactant-modified zeolite, Colloids Surf. A: Physicochem. Eng. Aspects 330 (2008) 35–41.
[14] A.M. Yusof, N.A.N. Nik Malek, Removal of Cr(VI) and As(V) from aqueous solutions by HDTMA-modified zeolite Y, J. Hazard. Mater. 162 (2009) 1019–1024.
[15] U. Wingenfelder, G. Furrer, R. Schulin, Sorption of antimonate by HDTMA-modified zeolite, Microporous Mesoporous Mater. 95 (2006) 265–271.
[16] Sh. Wang, W. Gong, X. Liu, B. Gao, Q. Yue, Removal of fulvic acids using the surfactant modified zeolite in a fixed-bed reactor, Sep. Purif. Technol. 51 (2006) 367–373.
[17] F. Akbal, Adsorption of basic dyes from aqueous solution onto pumice powder, J. Colloid Interface Sci. 286 (2005) 455–458.
[18] M. Kitis, S.S. Kaplan, E. Karakaya, N.O. Yigit, G. Civelekoglu, Adsorption of natural organic matter from waters by iron coated pumice, Chemosphere 66 (2007) 130–138.
[19] G. Neri, G. Rizzo, L. De Luca, F. Corigliano, I. Arrigo, A. Donato, Zeolitized-pumice as a new support for hydrogenation catalysts, Catal. Commun. 9 (2008) 2085–2089.
[20] A.N. Onar, B. Ozturk, Adsorption of phosphate onto pumice powder, Environ. Technol. 14 (1993) 1081–1087.
[21] F. Akbal, N. Akdemir, A.N. Onar, FT-IR spectroscopic detection of pesticides after sorption onto modified pumice, Talanta 53 (2000) 131–135.
[22] F. Akbal, Sorption of phenol and 4-chlorophenol onto pumice treated with cationic surfactant, J. Environ. Manage. 74 (2005) 239–244.
[23] S. Altenor, B. Carene, E. Emmanuel, J. Lambert, J.J. Ehrhardt, S. Gaspard, Adsorption studies of methylene blue and phenol onto vetiver roots activated carbon prepared by chemical activation, J. Hazard. Mater. 65 (2008) 1029–1039.
[24] B. Armagan, O. Ozdemir, M. Turan, M.S. Celik, The removal of reactive azo dyes by natural and modified zeolites, J. Chem. Technol. Biotechnol. 78 (2003) 725–732.
[25] K. Athanasiadis, B. Helmreich, Influence of chemical conditioning on the ion exchange capacity and on kinetic of zinc uptake by clinoptilolite, Water Res. 39 (2005) 1527–1532.
[26] J.J. Orfao, A.I. Silva, J.C. Pereira, S.A. Barata, I.M. Fonseca, P.C. Faria, Adsorption of a reactive dye on chemically modified activated carbons—influence of pH, J. Colloid Interface Sci. 296 (2006) 480–489.
[27] Gh. Ghanizadeh, G. Asgari, Adsorption kinetic and isotherm of methylene blue and its removal from aqueous solution using bone charcoal, React. Kinet. Mech. Catal. 102 (2011) 127–142.
[28] APHA, Standard Methods for the Examination of Water and Wastewater, 20th ed., 1998.

[29] M. Kitis, E. Karakaya, O.Y. Nevzat, G. Civelekoglua, A. Akcil, Heterogeneous catalytic degradation of cyanide using copper-impregnated pumice and hydrogen peroxide, Water Res. 39 (2005) 1652–1662.
[30] B. Ersoy, A. Sariisik, S. Dikmen, G. Sariisik, Characterization of acidic pumice and determination of its electrokinetic properties in water, Powder Technol. 197 (2010) 129–135.
[31] S.O. Maurice, M. Mike, O. Aoyi, O. Fred, Functionalised natural zeolite and its potential for treating drinking water containing excess amount of nitrate, Water SA 36 (2010) 123–130.
[32] M. Rožic, D. Ivanec Šipuši, L. Sekovanic, S. Miljanic, L.C. urkovic, J. Hrenovic, Sorption phenomena of modification of clinoptilolite tuffs by surfactant cations, J. Colloid Interface Sci. 331 (2009) 295–301.
[33] S.C. Sairam, N. Viswanathan, S. Meenakshi, Defluoridation chemistry of synthetic hydroxyapatite at nano scale: equilibrium and kinetic studies, J. Hazard. Mater. 155 (2008) 206–215.
[34] A.A.M. Daifullah, S.M. Yakout, S.A. Elreefy, Adsorption of fluoride in aqueous solutions using $KMnO_4$-modified activated carbon derived from steam pyrolysis of rice straw, J. Hazard. Mater. 147 (2007) 633–643.
[35] S. Jagtap, D. Thakre, S. Wanjari, S. Kamble, N. Labhsetwar, S. Rayalu, New modified chitosan-based adsorbent for defluoridation of water, J. Colloid Interface Sci. 332 (2009) 280–290.
[36] T.S. Anirudhan, M. Ramachandran, Surfactant-modified bentonite as adsorbent for the removal of humic acid from wastewaters, Appl. Clay Sci. 35 (2007) 276–281.
[37] N. Chena, Zh. Zhangb, Ch. Fenga, M. Li, D. Zhub, R. Chenb, N. Sugiurab, An excellent fluoride sorption behavior of ceramic adsorbent, J. Hazard. Mater. 183 (2010) 460–465.
[38] K. Biswas, K. Gupta, U. Chand Ghosh, Adsorption of fluoride by hydrous iron(III)–tin(IV) bimetal mixed oxide from the aqueous solutions, Chem. Eng. J. 149 (2009) 196–206.
[39] C. Sairam Sundaram, N. Viswanthan, S. Meenakhi, Fluoride sorption by nano-hydroxyapatite/chitin composite, J. Hazard. Mater. 172 (2009) 147–151.
[40] Y. Tangb, X. Guanc, J. Wanga, N. Gaob, M.R. McPhaild, Ch.C. Chusueid, Fluoride adsorption onto granular ferric hydroxide: effects of ionic strength, pH, surface loading, and major co-existing anions, J. Hazard. Mater. 171 (2009) 774–779.
[41] E. Kumarb, A. Bhatnagara, U. Kumarc, M. Sillanpaad, Defluoridation from aqueous solutions by nano-alumina: characterization and sorption studies, J. Hazard. Mater. 186 (2011) 1042–1049.
[42] L.M. Camacho, A. Torres, D. Saha, Sh. Deng, Adsorption equilibrium and kinetics of fluoride on sol–gel-derived activated alumina adsorbents, J. Colloid Interface Sci. 349 (2010) 307–313.
[43] K. Vasanth Kumar, S. Sivanesan, Selection of optimum sorption kinetics: comparison of linear and non-linear method, J. Hazard. Mater. 134 (2006) 277–279.
[44] A. Behnamfard, M.M. Salarirad, Equilibrium and kinetic studies on free cyanide adsorption from aqueous solution by activated carbon, J. Hazard. Mater. 170 (2009) 127–133.
[45] A. El Nemr, Potential of pomegranate husk carbon for Cr(VI) removal from wastewater: kinetic and isotherm studies, J. Hazard. Mater. 161 (2009) 132–141.
[46] J. Anwar, U. Shafique, M. Salman, W. Uz-Zaman, S. Anwar, J.M. Anzano, Removal of chromium(III) by using coal as adsorbent, J. Hazard. Mater. 171 (2009) 797–801.
[47] W.H. Cheung, Y.S. Szeto, G. McKay, Intraparticle diffusion processes during acid dye adsorption onto chitosan, Bioresour. Technol. 98 (2007) 2897–2904.